ELSEVIER

Nuclear Instruments and Methods in Physics Research B 190 (2002) 351–356

NIM B
Beam Interactions with Materials & Atoms

www.elsevier.com/locate/nimb

Micro-RBS characterisation of the chemical composition and particulate deposition on pulsed laser deposited $Si_{1-x}Ge_x$ thin films

A. Simon [a,*], Z. Kántor [b]

[a] *Institute of Nuclear Research of the Hungarian Academy of Sciences (ATOMKI), H-4001, P.O. Box 51, Debrecen, Hungary*
[b] *Research Group on Laser Physics of the Hungarian Academy of Sciences, Szeged, P.O. Box 406, H-6701, Szeged, Hungary*

Abstract

The formation and deposition of particulates by pulsed laser deposition of $Si_{1-x}Ge_x$ semiconductor alloy thin films are discussed. Using Rutherford backscattering spectrometry with micrometer lateral resolution (micro-RBS) the film composition was measured with high accuracy, even in the presence of particulates with a high areal density of 20,000–30,000 particulates per mm^2. We show that on impact of a particulate, the part of the thin film which is already deposited probably melts and its Ge content segregates to the surface. © 2002 Elsevier Science B.V. All rights reserved.

PACS: 82.80.Yc; 81.; 81.15.Fg; 68.35.Dv
Keywords: RBS; Microbeam; Pulsed laser deposition; Surface topography; Particulate formation

1. Introduction

In the last decade pulsed laser deposition (PLD) emerged as an important tool for thin film engineering [1]. In spite of many advantages, PLD has several drawbacks, which still hinder its wider application in large wafer microelectronics. There is theoretical and experimental evidence for the necessity of the different spatial distribution of the different elements in the plume and of the different sticking coefficients (deposition yield) of the different elements, different velocity vectors, surface quality and temperature. These effects result in an inhomogeneous film thickness and stoichiometry [1–4]. Another inevitable side-effect of PLD is the formation and deposition of particulates onto the substrate [5].

Although the droplet emission from the laser ablated surface can be investigated in situ by fast laser photography (see e.g. [6]), the only possibility for the determining how the individual particulates have been formed and deposited is ex situ morphological and chemical examination. Especially in case of Si–Ge materials, for the determination of the particulate composition, previous authors used energy dispersive spectroscopy (EDS) or Auger spectroscopy (AES) [2,7,8]. However, while the latter method reflects the composition of the outermost few nanometers, i.e. the thin film condensed after the deposition of the given particulate, EDS normally gives averaged information

* Corresponding author. Fax: +36-52-416181.
E-mail address: a.simon@atomki.hu (A. Simon).

0168-583X/02/$ - see front matter
PII: S0168-583X(02)00462-7

about the particulate and the thin film while the exact composition of the particulate itself remains unknown in both cases.

For the determination of the chemical composition of thin films, Rutherford backscattering spectrometry (RBS) is widely used as one of the most reliable techniques for quantitative analysis [2–4,9]. Since particulates represent layer thickness and composition inhomogeneities, they form a specific tail on the low-energy side of the peaks in the spectra representing the elements of the thin film. Therefore the evaluation of these spectra usually requires strict considerations and also complementary analyses [10]. The presence of some thousands of particulates per mm^2 is not unusual, and a considerable proportion of the surface may be covered by these particulates, so the reliability of the achievable composition information is often questionable using an ion millibeam.

Our previous experiences proved [11,12] that using a focussed MeV ion micro-beam combined with RBS provides reliable data in such cases. In this paper we demonstrate the determination of the PLD film composition using a micrometer lateral resolution RBS technique (micro-RBS), even if large amounts of particulates are present. We also present reliable measurements of the particulates' chemical composition and discuss the mechanism of their deposition.

2. Experimental details

The micro-RBS analyses were performed on a sample prepared by Antoni et al. [7,8]. The thin film was deposited using a sintered Si–Ge target with 20 at.% Ge fraction. An ArF excimer laser was used for ablation (193 nm wavelength, 20 ns pulse length) at 50 Hz repetition rate. The laser beam irradiated a 3×0.45 mm^2 area of the target at 45° angle of incidence. The substrate temperature was 600 °C during deposition, the ablating laser fluence and the number of shots were 4.6 J/cm^2 and 60,000, respectively. Before deposition, the $\langle 100 \rangle$ silicon substrate was cleaned with HF. The PLD chamber was evacuated to 10^{-7} mbar. The distance between the target and the substrate was 20 mm. The sample was characterized previously by a RBS millibeam, microbeam assisted energy dispersive X-ray spectroscopy (EDS) and Raman spectroscopy and these results were reported by Antoni et al. in Refs. [7,8].

Due to its high topographic resolution and large dynamic range [13,14], atomic force microscopy (AFM) is a suitable tool for the morphological characterisation of PLD generated thin films. The appearance of the droplets and their statistical characteristics (areal number density, surface coverage, total volume) were determined on AFM images recorded in the contact mode using a Topometrix Explorer TMX2000 equipment.

The micro-RBS measurements were performed at the Debrecen nuclear microprobe [15–17] using a 2.0 MeV $^4He^+$ beam of 2×2 μm^2 spot size. The beam current was measured by a beam chopper [18], all the RBS spectra were normalised to it, thus absolute elemental concentrations are calculated. The backscattered particles were detected by a Canberra PIPS detector of 50 mm^2 sensitive area and 14 keV energy resolution, set at 150° in IBM-geometry. Tomographic images were created by a computer code [11] while the RBS spectra were evaluated by the RBX computer code [19].

3. Results and discussion

Large-area AFM images showed that the typical particulate areal number density values vary between 19,000 and 34,000 mm^{-2} and ≈10–20% of the substrate surface is covered by different kinds of particulates. The lower values were observed at the outer areas where the film thickness is also smaller. Concerning the total volume of the particulates, its ratio to the film volume was of the order of 30%. The AFM images at higher magnifications showed many droplet-free zones up to 25 μm diameter are distributed over the surface. Thus even under such extreme conditions, μRBS must be able to determine the composition of the film with high confidence [12].

Four different basic types of particulates are distinguished by the AFM topographic images and illustrated in Fig. 1. Type 1: disc-shaped circular splashes with thicker edge; their typical thickness

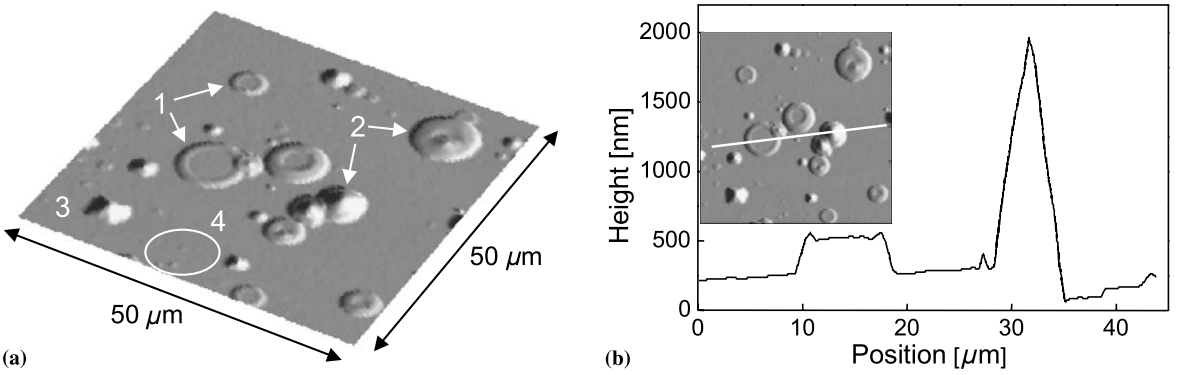

Fig. 1. (a) AFM image of a 50×50 μm^2 area of the PLD film and (b) a height profile along the line indicated in the inset. Four different basic types of particulates are distinguished and illustrated.

being between 100 and 400 nm. The diameter of such particulates varies between 5 and 30 μm (larger species have also been observed). Type 2: 5–25 μm broad features with thick edge and even thicker part ("peak") in the centre (hundreds of nm and >1 μm, respectively). Type 3: micron-high and wide droplets or fragments, not resolved by the AFM, rather replicating the square-base pyramid shape of the AFM tip. Type 4: small particulates, also indicated but not resolved by AFM. Further, on some AFM images we observed areas from where the film has apparently been removed due to particulate impact.

A typical RBS spectrum of a 100×100 μm^2 area is shown in Fig. 2. The Ge content of the thin film is represented by a peak at backscattered ion energies below 1632 keV (ch. 434, Ge high-energy edge). Ge counts originating below 1536 keV (ch. 408; depending on the actual film thickness) can only be present due to larger stopping than is possible within the condensed thin film, i.e. either due to additional stopping within the particulate volume, or diffusion of germanium into the underlying silicon substrate. Since the latter effect was negligible at the processing substrate temperature of 600 °C, these counts can solely be attributed to the Ge content of the particulates. In order to distinguish the regions covered by the particulates from the droplet-free areas, we analysed the lateral distribution of backscattered ions belonging to the energy window between ch. 320 and 390 (see Fig. 3(a)) where a germanium elemental map of a

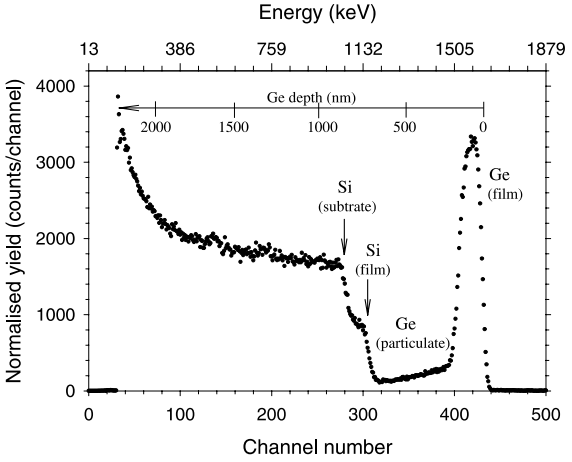

Fig. 2. A typical RBS spectrum of a 65×65 μm^2 area (2 MeV He^+, $\Theta = 150°$). The backscattered particles from Ge incorporated into the thin film and particulates are well distinguished.

65×65 μm^2 area is shown, but distinguishing between the different types of particulates requires the analysis of tomographic images like the one in Fig. 3(b). It can be seen clearly that the Ge depth distribution of the particulate in the left side reduces within a shallow depth range revealing that this object is a type 3 particulate, in contrast to the type 2, which possesses Ge content distributed deeper than a micron. Particulates of type 4 may be covered by one or two pixels in the elemental map with certain probability.

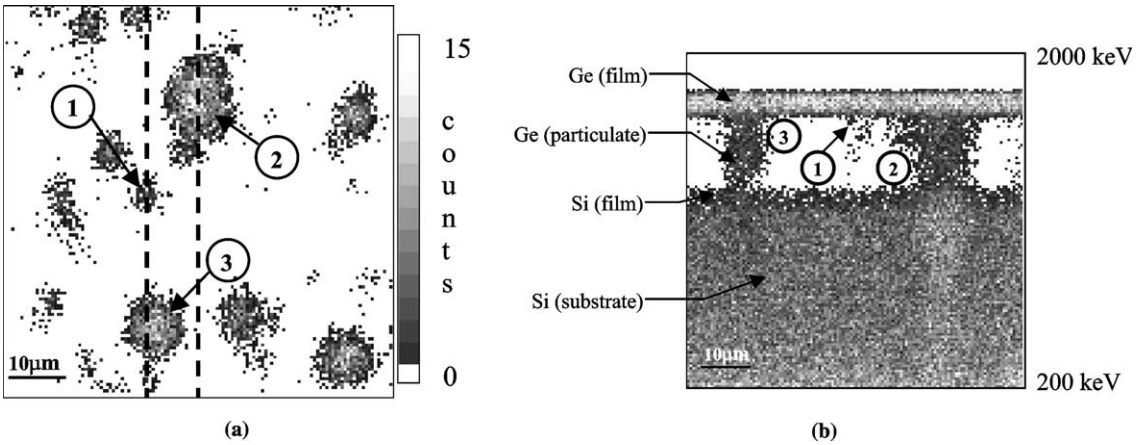

Fig. 3. (a) Ge elemental map (energy window between ch. 320 and 390, 65×65 μm^2 scanning area, 128×128 pixel), (b) tomographic image created from 15 pixels wide region between the vertical lines. The different types of particulates characterised in Fig. 1. are also represented. For discussion see text.

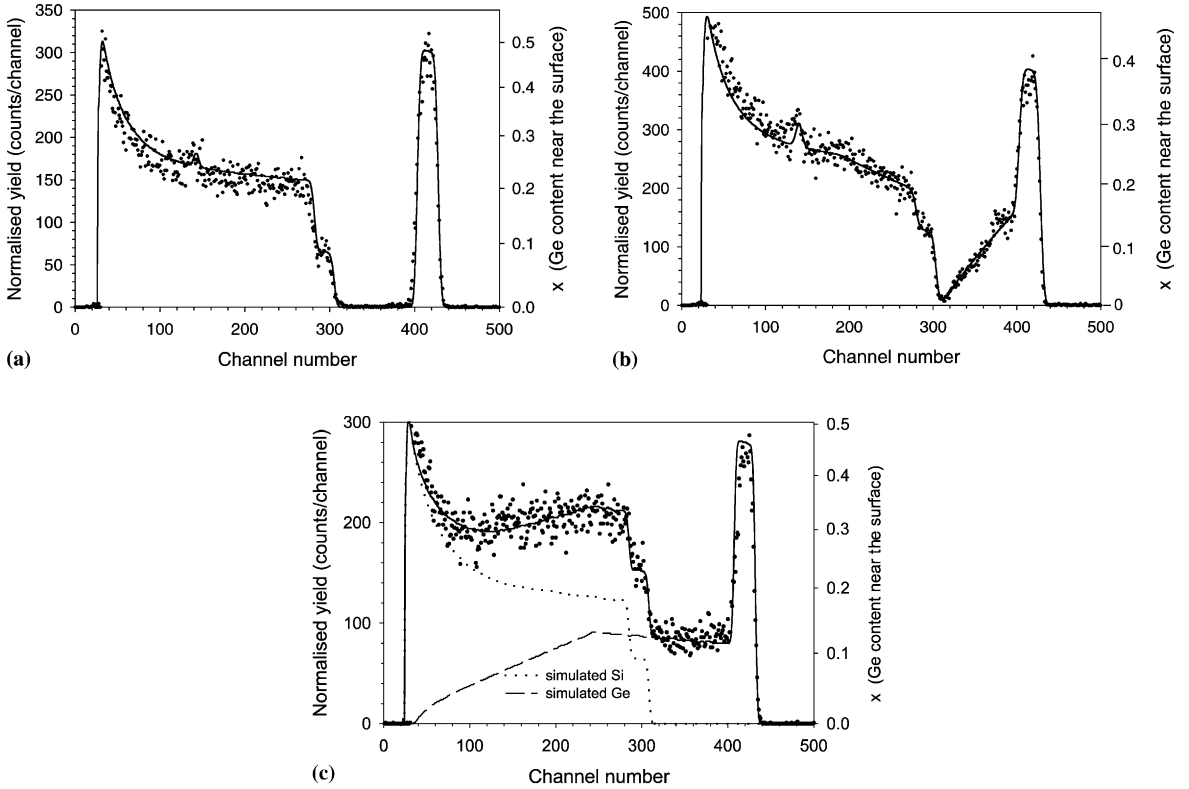

Fig. 4. RBS spectra (dots: measured; lines: simulated) collected on a (a) particulate-free area (160 nm nominal film thickness, $x = 0.48$), (b) 640 nm thick particulate (x linearly changes from zero to 0.14 toward the surface) covered by a 165 nm thick ($x = 0.38$) film, (c) 2300 nm thick particulate with $x = 0.12$ Ge content in the upper part and decreasing one toward the substrate as the subspectra show, covered by a 165 nm thick ($x = 0.46$) film. The extra counts below ch. 390 are characteristic for the Ge content of the particulate. (The thin carbon film (ch. 155) is due to the poor vacuum conditions and long measuring times.)

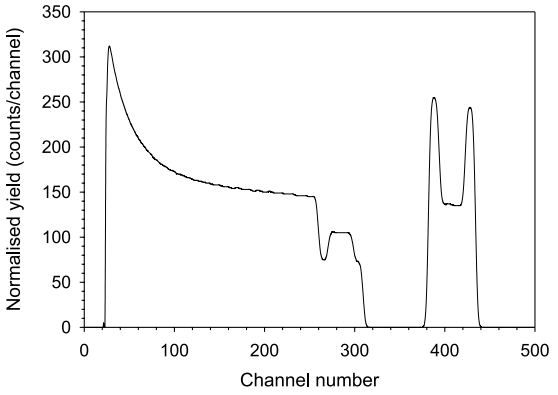

Fig. 5. Simulated RBS spectrum of a hypothetical $Si_{1-x}Ge_x$ multilayer structure: 75 nm with $x = 0.4$ / 200 nm with $x = 0.2$ / 75 nm with $x = 0.4$ / silicon substrate. The different Ge contents are well separated in the Ge peak. Please note the decreased Si yield around ch. 265 because of the Ge content of the underlying film.

The composition of the thin PLD film was determined by evaluating the micro-RBS spectra collected by point scan mode. A typical point spectrum is shown in Fig. 4(a), which reveals the presence of a thin film with 48 at.% Ge content only, without any signs of droplets. Further point spectra, Fig. 4(b) and (c), were collected on the centre of particulates. As it was found that there is a distribution of the Ge elemental concentration in depth, for more precise calculation the layer was split into 100 slices of the same thickness and linearly graded Ge profile.

Regarding the mechanism of the deposition and solidification of the film in the PLD, one would expect that each droplet is enclosed between the two parts of the thin layers which condensed before and after the deposition of a droplet. According to our measurement of the thin film composition (some 40 at.% Ge fraction) and assuming that the droplet composition matches that of the target [2] (20 at.% Ge), for type 1 particulates one would expect RBS spectra similar to that in Fig. 5. However, such structures were not found *at all*, in any of the investigated areas. Typically, as shown in Fig. 4(b) and (c) a Ge rich upper layer was found on the surface, and underneath this film another layer was observed with low (≈14 at.%) Ge content just at the interface and even rapidly decreasing Ge fraction toward the substrate. To emphasise, after measuring several tens of spectra on droplets in different areas we have not found such high Ge-content region beneath the droplet material, at all. It is rather unlikely that all the analysed particulates would have been deposited before the film has reached a thickness detectable by RBS, especially because particulate formation is normally continuously enhanced upon durable ablation of the target surface due to the increased roughness [5].

A plausible explanation of the absence of the PLD layer beneath the droplet is that due to the high temperature of the arriving droplet, the existing film melted and mixed with the droplet material. As the substrate extracted heat from the molten material, solidification is set on first at the interface and gradually toward the free surface. Upon the movement of the solidification front, the germanium most likely moves towards the surface [20], resulting in a continuously increasing Ge content. During this process it is not necessary that the underlying silicon melts, since (i) it always has a higher melting point than any alloy of germanium and silicon, and (ii) the thermal contact of the PLD layer to the surface may be incomplete. The manifestation of the incomplete interface is illustrated by the thin film parts removed upon particulate impact also observed in the AFM images.

It is also worth noting that the material in the volume of the resolidified particulates has a significantly lower average atomic Ge fraction than the original target material. If the above described mechanism works, then the composition of the resolidified droplet may have little relation to that of the original target material. This conclusion is not in accordance with that of Arnold and Aziz [2] who found an equivalence between target and droplet composition by electron microprobe analysis of the droplets and macro-RBS analysis of the target. Furthermore, because of the depth dependence of the Ge distribution, electron beam assisted methods like AES [8] or EDS [2,7,8] are not suitable for the characterisation of the composition of the material carried by the particulates, since the first method possesses too small sampling depth which accesses only the condensed thin film

itself, while the latter one provides averaged information over a thick region including the thin film and particulates.

Our experimental data are not sufficient to estimate the total Si–Ge balance of the overall PLD process including particulate formation, but it seems rather likely that the Si–Ge target is not ablated congruently; after melting at significantly lower temperatures than the underlying Si rich zone, the Ge rich upper layer evaporates first, and then the emission of the Si-rich droplets takes place.

4. Conclusions

The micro-RBS technique proved to be able to determine the chemical composition and depth distribution of thin PLD films even if a considerable proportion of the surface is covered by particulates. The layer deposited via laser evaporation of a $Si_{0.8}Ge_{0.2}$ target contains typically 35–48 at.% Ge. The chemical composition of the droplets can not be characterised by a single number. From the substrate to the surface, the Ge content of the particulates increases from practically zero to ≈12–14%, revealing a Ge segregation effect upon solidification.

Acknowledgements

This work was supported by the Hungarian Scientific Research Fund (OTKA T34381). A. Simon and Z. Kántor are thankful to the Hungarian Academy of Sciences for their Bolyai János Postdoctoral Scholarship.

References

[1] D.B. Chrisey, G.K. Hubler (Eds.), Pulsed Laser Deposition of Thin Films, Wiley, New York, 1994.
[2] C.B. Arnold, M.J. Aziz, Appl. Phys. A 69 (1999) S23.
[3] J. Perrière, in: E. Fogarassy, S. Lazare (Eds.), Laser Ablation of Electronic Materials, Elsevier Science, Amsterdam, 1992, p. 293.
[4] J. Gonzalo, C.N. Afonso, F. Vega, D. Martínez García, J. Perrière, Appl. Surf. Sci. 86 (1995) 40.
[5] L.C. Chen, Particulates generated by pulsed laser ablation, in: D.B. Chrisey, G.K. Hubler (Eds.), Pulsed Laser Deposition of Thin Films, Wiley, New York, 1994, p. 167.
[6] T. Smausz, B. Hopp, Cs. Vass, Z. Tóth, Appl. Surf. Sci. 168 (2000) 146.
[7] F. Antoni, E. Fogarassy, C. Fuchs, B. Prévot, J.P. Stoquert, Appl. Surf. Sci. 86 (1995) 175.
[8] F. Antoni, E. Fogarassy, C. Fuchs, J.J. Grob, B. Prévot, J.P. Stoquert, Appl. Phys. Lett. 67 (1995) 2072.
[9] A.R. Ramos, O. Conde, F. Pászti, G. Battistig, É. Vázsonyi, M.R. da Silva, M.F. da Silva, J.C. Soares, Nucl. Instr. and Meth. B 161–163 (2000) 926.
[10] J. Slotte, A. Laakso, T. Ahlgren, E. Rauhala, R. Salonen, J. Räisänen, A. Simon, I. Uzonyi, Á.Z. Kiss, E. Somorjai, J. Appl. Phys. 87 (1) (2000) 140.
[11] A. Simon, Z. Kántor, I. Rajta, T. Szörényi, Á.Z. Kiss, Nucl. Instr. and Meth. B 181 (2001) 360.
[12] Z. Kántor, T. Szörényi, Zs. Tóth, A. Simon, L. Gombos, Appl. Surf. Sci. 138–139 (1999) 599.
[13] Á. Mechler, P. Heszler, C.T. Reimann, K. Révész, Z. Bor, Vacuum 50 (3–4) (1998) 281.
[14] P. Heszler, K. Révész, C.T. Reimann, Á. Mechler, Z. Bor, Nanotechnology 11 (2000) 37.
[15] I. Rajta, I. Borbély-Kiss, Gy. Mórik, L. Bartha, E. Koltay, Á.Z. Kiss, Nucl. Instr. and Meth. B 109/110 (1996) 148.
[16] Z. Elekes, I. Uzonyi, B. Gratuze, P. Rózsa, Á.Z. Kiss, G. Szöőr, Nucl. Instr. and Meth. B 161–163 (2000) 836.
[17] Z. Elekes, Á.Z. Kiss, Gy. Gyürky, E. Somorjai, I. Uzonyi, Nucl. Instr. and Meth. B 158 (1999) 209.
[18] L. Bartha, I. Uzonyi, Nucl. Instr. and Meth. B 161–163 (2000) 339.
[19] E. Kótai, Nucl. Instr. and Meth. B 85 (1994) 588.
[20] R. Reitano, P.M. Smith, M.J. Aziz, J. Appl. Phys. 76 (1994) 1518.